JGR Space Physics

RESEARCH ARTICLE
10.1029/2020JA028854

# Diurnal UT Variation of Low Latitude Geomagnetic Storms Using Six Indices

**N. Balan[1], S. Tulasi Ram[2], V. Manu[1], Lingxin Zhao[1], Zan-Yang Xing[1], and Qing-He Zhang[1]**

[1]Institute of Space Sciences, Shandong University, Weihai, China, [2]Indian Institute of Geomagnetism, Navi Mumbai, India

**Key Points:**

- A striking quasi-semidiurnal pattern is observed in the UT distribution of the geomagnetic storm intensity in six low latitude indices
- Similar pattern exists in the UT variation of the computed value of the main energy input in the ring current
- The quasi-semidiurnal pattern correlates well with the angles $\mu$ and $\theta$ involved in the mechanisms of equinoctial hypothesis and RM effect

**Supporting Information:**

Supporting Information may be found in the online version of this article.

**Correspondence to:**

N. Balan,
balan.nanan@yahoo.com

**Citation:**

Balan, N., Ram, S. T., Manu, V., Zhao, L., Xing, Z.-Y., & Zhang, Q.-H. (2021). Diurnal UT variation of low latitude geomagnetic storms using six indices. *Journal of Geophysical Research: Space Physics*, *126*, e2020JA028854. https://doi.org/10.1029/2020JA028854

Received 28 OCT 2020
Accepted 20 SEP 2021

**Abstract** A quasi-semidiurnal type pattern was observed earlier in the diurnal UT variation of the geomagnetic storms studied using mainly Kyoto Dst (disturbance storm-time) index. However, the pattern has been argued as apparent due to uneven longitude distribution of the four Dst observatories. Unlike earlier studies, this paper investigates the diurnal UT variation of the storms automatically identified in six available indices including Kyoto Dst, USGS (United States Geological Survey) Dst, SymH (symmetric-H), RC (ring current), Dcx (corrected extended Dst), and AER (Atmospheric and Environmental Research) in 50, 50, 36, 21, 5, and 7 years, respectively. The indices are derived using 4, 4, 12, 14, and 15 ground observatories (with maximum longitude separations of ~120°, 120°, 70°, 110°, and 50°) and four DMSP (Defense Meteorology Satellite Program) satellites, respectively. The UT distribution of the storm intensity (minimum value of an index during the storm main phase) in all indices shows a striking quasi-semidiurnal type variation with maxima around 06–08 UT and 21–23 UT and minima around 03–05 UT and 13–15 UT. Similar quasi-semidiurnal variation is also observed in the computed values of the main energy input in the ring current. The variation correlates well with the variations of the dipole tilt angles $\mu$ and $\theta$ involved in the equinoctial hypothesis and Russell-McPherron (RM) effect, respectively. These observations indicate that the quasi-semidiurnal variation is real.

**Plain Language Summary** Large disturbances in the geomagnetic field lasting form several hours to several days are known as geomagnetic storms. The variations of the occurrence and intensity of the storms with solar activity and season have been understood thanks to the works of a large number of scientists. The variation of the storms with the time-of-day studied using mainly the low latitude geomagnetic activity index Dst has shown a quasi-semidiurnal pattern. The pattern, however, has been argued as apparent due to the uneven longitude distribution of the four magnetic observatories used for deriving Dst. The present study investigates the diurnal UT variation of the storms using six available indices. The results show similar striking quasi-semidiurnal patterns in the UT distribution of the storm intensity in all indices and computed value of the main energy input in the ring current. The quasi-semidiurnal pattern also correlates well with the angles $\mu$ and $\theta$ involved in the mechanisms of equinoctial hypothesis and RM effect. These observations indicate that the quasi-semidiurnal variation is real.

## 1. Introduction

Large disturbances in the geomagnetic field lasting from several hours to several days are known as geomagnetic storms. The storms are characterized by enhanced magnetospheric and ionospheric current systems (e.g., Akasofu, 1981; Gonzalez et al., 1994; Lühr et al., 2017; Svalgaard, 1977). The various current systems, however, contribute to cause different ground magnetic field disturbances (or geomagnetic storms) at different latitudes. Therefore, the storms at low, mid, and high latitudes are usually represented by the indices such as Dst (disturbance storm-time), Kp, and AE, respectively (Love & Gannon, 2009; Rostoker et al., 1995; Sugiura, 1964). The storms at low latitudes arise mainly from the enhanced solar wind-magnetosphere coupling and ionosphere-ring current coupling due to solar storms (e.g., Daglis, 1997; Ebihara et al., 2005). The geomagnetic data, indices, and models have been used to study the storms for over 150 years in numerous papers (e.g., Burton et al., 1975; Iyemori, 1980; Katus & Liemohn, 2013; Liemohn et al., 2001; Lockwood, McWilliams, et al., 2020; Lockwood, Owens, et al., 2020; Sabine, 1856; Vijaya Lekshmi et al., 2011). The results indicate that the occurrence and intensity of the storms (observed mainly in Dst) undergo solar cycle, annual, and diurnal variations. Here, storm intensity is defined as the maximum negative value of an index during the storm main phase (MP), which is denoted by DstMin for the Dst index.

With solar cycle, the storms become more frequent and more intense with increasing level of solar activity (e.g., Ellis, 1899; Zhang et al., 2007), as expected from the frequent occurrence of faster CMEs (coronal mass ejections) and ICMEs (interplanetary CMEs) at higher levels of solar activity (e.g., Gopalswamy et al., 2005). During solar minimum, weak recurrent storms are observed frequently due to the interaction of the corotating interaction regions (CIRs) of solar origin with the magnetosphere (e.g., Richardson et al., 2001; Tulasi Ram et al., 2010). The annual variation is characterized by a semiannual pattern with equinoctial maxima and solstice minima (e.g., Svalgaard, 2011; Zhao & Zong, 2012). The semiannual variation has been explained using the axial hypothesis (e.g., Cortie, 1912), equinoctial hypothesis (e.g., Azpilicueta & Brunini, 2012; Bartels, 1932) and Russell-McPherron (RM) effect (Russell & McPherron, 1973), the latter two mechanisms involving solar wind-magnetosphere coupling. The equinoctial hypothesis is based on the varying tilt angle $\mu$ between the Earth's dipole axis and GSE (geocentric solar ecliptic) $Z$-axis in the $X$-$Z$ plane where the $X$ points toward the center of the Sun from the center of the Earth. On the other hand, the RM effect is based on the varying tilt angle $\theta$ of the dipole axis with respect to GSEQ (geocentric solar equatorial) $Z$-axis in the plane perpendicular to the Sun-Earth line. Newell et al. (2001) and Lyatsky et al. (2001) suggested that the simultaneous drift of both auroral ovals from the dayside to the nightside at equinoxes can contribute to the semiannual variation. Recently, Lockwood, McWilliams, et al. (2020) and Lockwood, Owens, et al. (2020) compared the semiannual variation of the geomagnetic data (Dst, high latitude, and global indices) with corresponding variation in the power input into the magnetosphere (Pa) estimated from interplanetary observations. They found that the semiannual variation in the geomagnetic data is amplified compared to that in Pa and the amplification is maximum (~10 times) in Dst.

The diurnal universal time (UT) variation of the geomagnetic storms in different indices has been reported in a number of papers (e.g., Mayaud, 1978; Saroso et al., 1993; Siscoe & Crooker, 1996; Takalo et al., 1995). The non-Dst indices generally exhibit a diurnal UT variation. For example, Lockwood, McWilliams, et al. (2020); Lockwood, Owens, et al. (2020) showed that the planetary index *am* exhibits a diurnal UT variation with maximum/minimum at ~21–24/03–06 UT, which as they discussed is a real feature of geomagnetic activity. The low latitude Dst index, however, has shown a quasi-semidiurnal variation. Using about 220 Dst storms of DstMin $\leq -50$ nT in 1966–1987, Ahn et al. (2002) reported that the Dst value is about 23% lower than the daily mean at around 07 UT and 28% higher at around 12 UT during the main phase (MP) of the storms. The observed quasi-semidiurnal variation of the storms (e.g., Saroso et al., 1993) has been interpreted as real in terms of the equinoctial hypothesis (Bartels, 1932) and RM effect (Russell & Mcpherron, 1973). It has also been argued as apparent due to the uneven longitude and latitude distributions of the four Dst stations (e.g., Mayaud, 1978; Takalo & Mursula, 2001). Recently, Yakovchouk et al. (2012) studied the average properties of the storms (DstMin $\leq -50$ nT) in 1932–2009 (Karinen & Mursula, 2005) using the global and local Dxt indices derived from the data at the four Dst stations. They found that the local Dxt minima occur at around 18 LT (local time), the minima are typically 25–30% stronger than the global Dxt minimum, and the (UT) time of the global Dxt minimum is mostly determined by the UT hour of the maximum disturbance at ~18 LT in one of the Dst stations.

As introduced, mainly Kyoto Dst has been used before for studying the diurnal UT variation of the geomagnetic storms at low latitudes, and the quasi-semidiurnal variation observed in the index has been argued as apparent due to the uneven longitude distribution of the four Dst stations. In the present paper, we investigate the diurnal UT variation of the low latitude geomagnetic storms in six indices computed using data from 4 to 15 ground stations and four satellites. The indices include the widely used Kyoto Dst (Sugiura, 1964), new and improved USGS Dst (Love & Gannon, 2009), SymH index (Iyemori et al., 1992), RC (ring current) index (Olsen et al., 2005), and Dcx (corrected extended Dst) index (Karinen & Mursula, 2005) computed using ground stations, and AER (Atmospheric and Environmental Research) index computed using data from four DMSP (Defense Meteorology Satellite Program) satellites.

Figure 1 is an example of the storm in the six indices on March 17, 2015. It illustrates that the important storm characteristics such as MPO (main phase onset) and storm intensity (minimum value of an index during the main phase) occur at the same UT hour in all indices within their time resolutions. It will be shown (Section 4) that the UT distribution of the storm intensity in all indices exhibits a striking quasi-semidiurnal type variation irrespective of the indices being satellite-based or ground-based and the number of observatories used and their longitude separations. Similar quasi-semidiurnal variation is also observed

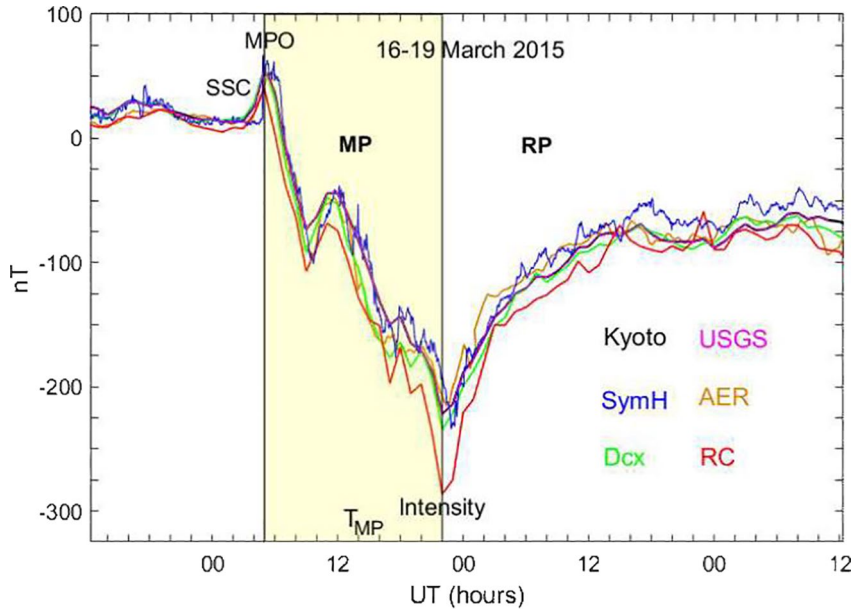


**Figure 1.** Example of a storm in six indices on March 17, 2015. The main phase onset (MPO), storm intensity, and main phase duration $T_{MP}$ are noted.

in the computed values of the energy input in the ring current. The quasi-semidiurnal variation also correlates well with the angles $\mu$ and $\theta$ involved in the mechanisms of equinoctial hypothesis and RM effect. These observations indicate that the quasi-semidiurnal variation is real, probably caused by the physical mechanisms such as equinoctial hypothesis or Russell-McPherron (RM) effect or their combination. This conclusion could stimulate the scientific community to continue studying this interesting topic further using data and models.

The six indices are briefly described in Section 2. The storms automatically identified by a computer program (Balan, Tulasiram, et al., 2017; Balan, Zhang, Xing, et al., 2019) are analyzed in Section 3. Since large number of years of data are needed to remove statistical fluctuations (Russell & McPherron, 1973), we use the widely used Kyoto Dst and new and improved USGS Dst available for the long 50-year period to investigate the UT occurrence of the storm intensity in different seasons and solar cycles. These indices are also used to study the UT variation of the computed values of the main energy input in the ring current during the storm main phase (Burton et al., 1975). In addition, the combined time-of-year/time-of-day plots simultaneously connecting the annual and diurnal UT distributions of the stormy hours when Dst $\leq -50$ nT are also presented for these indices.

## 2. Data and Availability

Sugiura (1964) computed the Kyoto Dst index from the H-component magnetic field measured at four low latitude observatories (three in northern hemisphere and one in southern hemisphere) having maximum longitude separation (MLS) of ~120°. The hourly Dst index of 1 nT resolution is available since 1957 at http://wdc.kugi.kyoto-u.ac.jp/dstdir/. Love and Gannon (2009) produced the USGS Dst following the same calculation algorithm of Sugiura (1964). However, they employed more robust time and frequency domain band-stop filtering to remove the specific periodic terms corresponding to the rotation of the Earth and solar and lunar tidal components. The hourly USGS Dst of 0.1 nT resolution is available since 1958 at http://geomag.usgs.gov/data. Details about the computations of the two indices can be found in Sugiura and Kamei (1991) and Love and Gannon (2009).

The SymH index (Iyemori et al., 1992) is similar to Kyoto Dst but computed using the H-component data from up to 12 low and midlatitude stations (10 in the north and 2 in the south) of MLS ~70°. It has 1-min resolution and is available since 1981 at http://wdc.kugi.kyoto-u.ac.jp/aeasy. The RC index (Finlay et al., 2012;

**Table 1**
*Lists the Indices Including the Number of Ground Stations (or Satellites) Used for Them and the Maximum Longitude Separation (MLS) Between the Stations, Years of Indices Used, Number of Storms, and Their Diurnal Means and Mean Quasi-Semidiurnal Maxima and Minima in Percentage of the Diurnal Means*

| Index | No. of stations | MLS (°) | Years of data | No. of storms | Diurnal mean | Diurnal max (%) | Diurnal min (%) |
|---|---|---|---|---|---|---|---|
| Kyoto | 4 | 120 | 50 | 761 | 31.7 | 75 | 50 |
| USGS | 4 | 120 | 50 | 585 | 24.4 | 58 | 45 |
| RC | 14 | 110 | 21 | 258 | 10.7 | 142 | 90 |
| SymH | 12 | 70 | 36 | 535 | 22.3 | 50 | 33 |
| Dcx | 14 | 50 | 5 | 61 | 2.5 | 92 | 68 |
| AER | Four satellite | Satellite | 7 | 97 | 4.0 | 37 | 33 |

Olsen et al., 2005) is similar to Kyoto Dst but uses the H-component data from 14 low and midlatitude stations (11 in the north and 3 in the south) of MLS ~110°. It is available since 1997 at http://www.spacecenter.dk/files/magnetic-models/RC/. Karinen and Mursula (2005) produced a corrected extended version of Dst (Dcx) index extending back to 1932. Recently, they produced a new version of Dcx using 15 low and midlatitude stations (10 in the north and 5 in the south) of MLS ~50°. We use this version of Dcx available since May 2013 at http://dcx.oulu.fi/?link=queryProvisional. The AER index having 12.75-min resolution is a US-based space-based real-time alternative to Kyoto Dst. It uses the H-component data from four DMSP (Defense Meteorology Satellite Program) satellites and is available since March 2011 at https://www.aer.com/science-research/space/space-weather/space-weather-index/. The indices, however, have significant differences (Figure 1) mainly due to the different methods of removal of the secular and Sq (solar quiet) variations calculated in different ways in different indices (e.g., Love & Gannon, 2009; Sugiura & Kamei, 1991). The differences, however, do not affect the purpose of the study because the storm intensity occurs at the same UT hour in all indices (Figure 1).

## 3. Storm Identification and Analysis

The storms in all indices are automatically identified by a computer program that applies four selection criteria that minimize nonstorm-like fluctuations. The criteria are (a) storm intensity ≤−50 nT and storm main phase (MP) duration $T_{MP} > 2$ h, (b) absolute value of MP range (e.g., $|Dst_{MPO} - DstMin|$) ≥ 50 nT, (c) separation between storm intensity and next MPO ≥ 10 h, and (d) rate of change of an index during MP (e.g., $(dDst/dt)_{MP}$) < −5 nT $h^{-1}$. Details about the storm identification explained in Balan,Tulasiram, et al. (2017) and Balan, Zhang, Xing, et al. (2019) are not repeated here. The program identified a total of 761 and 585 storms in Kyoto Dst and USGS Dst, respectively, during the period from 1958 to 2007 (Table 1 and Table S1 and Table S2). The number of storms in Kyoto Dst is 176 more than those in USGS Dst. The difference is mainly due to the fixed threshold considered (DstMin ≤ −50 nT) as discussed in Balan, Zhang, Xing, et al. (2019). The number of storms identified (Table 1) in SymH is 535 in 1981–2017, RC is 258 in 1997–2017, AER is 97 in 2011–2017, and Dcx is 61 in 2013–2017. The storms in Kyoto Dst have been used to develop a scheme for forecasting severe space weather causing electric power outage and telecommunication failure (Balan et al., 2014, Balan, Ebihara, et al., 2017) and investigating the corresponding ionosphere-thermosphere storms and low latitude aurora (Balan, Zhang, Shiokawa, et al., 2019).

The storms are analyzed for their important parameters. MPO is main phase onset; it is also the peak of SSC (storm sudden commencement, Figure 1). The minimum value of an index during main phase (MP) is the storm intensity. The time interval between MPO and time of occurrence of the storm intensity (DstMin) is the main phase duration $T_{MP}$. The UT hours of MPO and storm intensity in all indices are noted. The Dst data are also used to calculate the rate of ring current development $E$ (Burton et al., 1975), defined as

$$E = \left(\frac{d\mathrm{Dst}}{dt}\right)_{\mathrm{MP}} + \alpha \mathrm{Dst}_{\mathrm{MP}}.$$

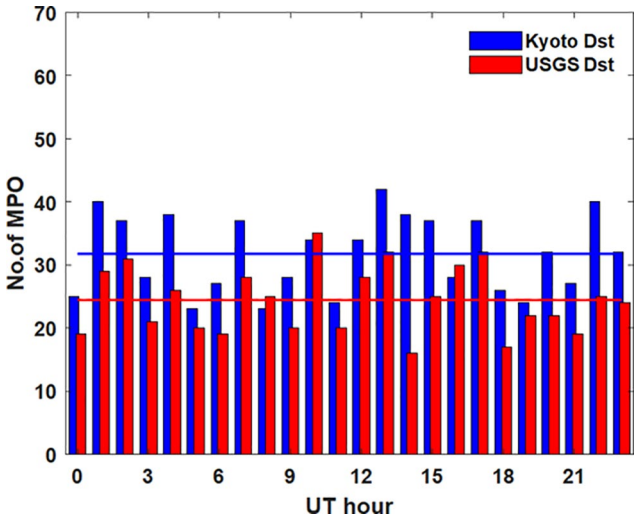


**Figure 2.** Overall diurnal universal time (UT) variation of hourly number of main phase onset (MPO) of the storms in Kyoto Dst (blue) and USGS Dst (red); horizontal lines represent diurnal means.

Here, $\alpha = 0.13$/hour is the ring current decay constant corresponding to the decay time of 7.7 hr obtained by investigating the effects of the variations in the parameters involved in the original Burton equation (e.g., Burton et al., 1975; O'Brien & McPherron, 2000, 2002). Several other studies also investigated the decay time and its dependence on other parameters like solar wind velocity ($V$) and IMF Bz. However, in the present study, we consider the value of the decay time as 7.7 hr following Burton et al. (1975), which is widely accepted in the literature. $(\mathrm{dDst/d}t)_{\mathrm{MP}}$ is the rate of change of Dst during MP calculated as the difference between the two successive Dst values from MPO to DstMin; its maximum value is $(d\mathrm{Dst}/dt)_{\mathrm{MPmax}}$. $\mathrm{Dst}_{\mathrm{MP}}$ in the second term is the mean of the two successive Dst values used for the calculating the first term. Since the main energy input in the ring current from solar wind takes place during MP and Dst is mainly a ring current index, the rate of the ring current development $E$ is considered proportional to the rate of energy input in the ring current.

## 4. Results

Diurnal UT variations of the distribution of DstMin and $E$ (energy input) are presented for the 50-year long Kyoto Dst and USGS Dst. For other indices, the UT distribution of the storm intensity alone is presented; number of storms is not sufficient to obtain the average value of $E$ to study its UT variation.

### 4.1. Storm Statistics in Dst Indices

The storms in each UT hour in 1958–2007 are combined to obtain the overall diurnal UT distribution of the storm main phase onset (MPO) and storm intensity (DstMin). It gives 24-point data series from 00 to 23 UT. Figure 2 shows the resulting UT variation of the hourly distribution of MPO in both versions of Dst. Horizontal lines indicate the diurnal means. MPO has nearly uniform UT distribution, except for short-period fluctuations, as expected from the noncorrelation of the solar wind (and IMF) driver of geomagnetic storms with the phase of Earth's rotation. The irregular short-period fluctuations could most probably be due to the time resolution of the data (1 hr). That is, storms occurring at approximately one hour apart (at $X$:00 and $X$:59 UT) are considered to belong to the same hour ($X$ UT). The variations in the small-time interval between the impact of the solar wind driver at the magnetopause and development of MPO also might contribute to the small fluctuations.

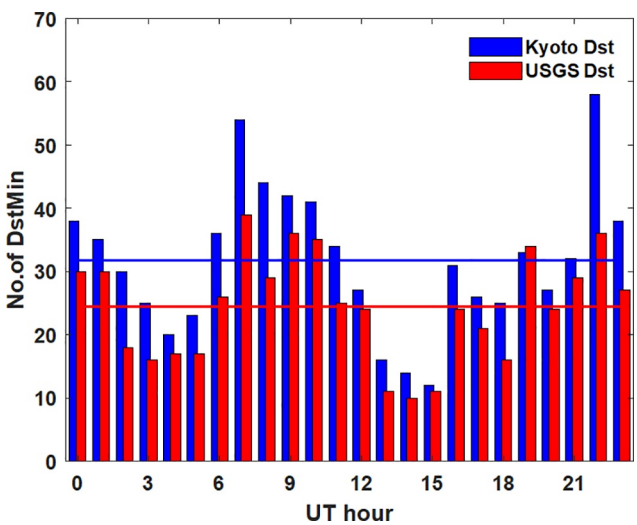


**Figure 3.** Overall diurnal universal time (UT) variation of hourly number of DstMin of the storms in Kyoto Dst (blue) and USGS Dst (red); horizontal lines represent diurnal means.

Figure 3 shows the UT variation of the hourly distribution of DstMin in both versions of Dst. The horizontal lines indicate diurnal means. Unlike in the distribution of MPO, the striking feature in the distribution of DstMin (Figure 3) is a quasi-semidiurnal type variation. In both versions of Dst, the distribution of DstMin exhibits maxima around 06–08 UT and 21–23 UT and minima around 03–05 UT and 13–15 UT. Considering the two indices together, the average maxima and average minima are found to be ~65% and −48% of their diurnal means (Table 1), respectively. The small fluctuations could most probably be due to the time resolution of the data (1 hr) as discussed above (Figure 2). Since the two maxima and minima are not separated by 12 hr and their amplitudes are different, we call the observed variation quasi-semidiurnal. The location of the two minima (03–05 UT and 13–15 UT) are in Atlantic and Pacific where there is only one station (Honolulu) in Kyoto Dst and USGS Dat. However, it does not seem to affect the quasi-semidiurnal variation as will

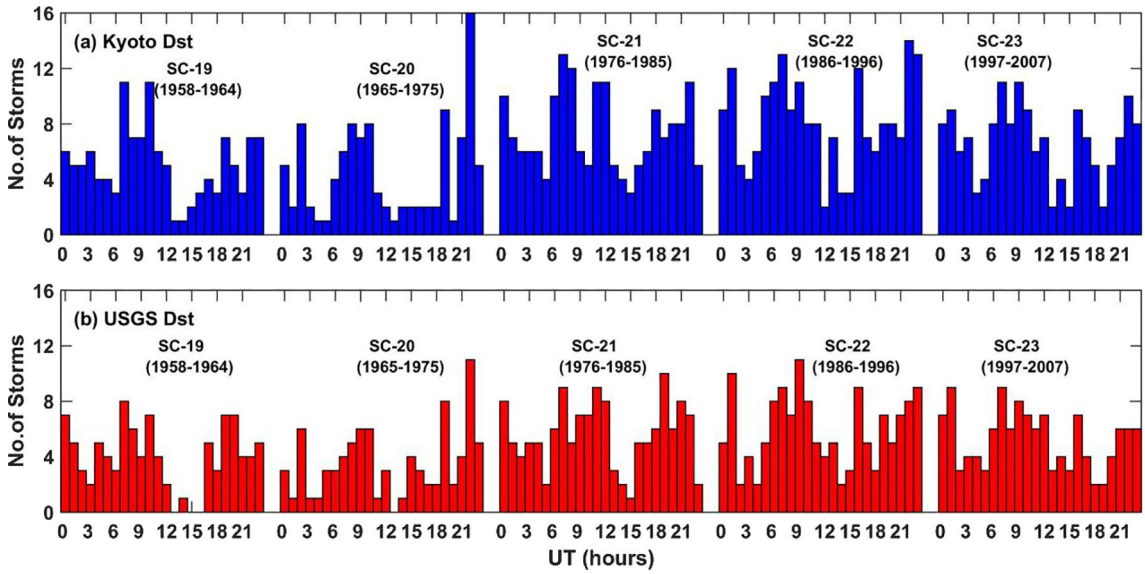


**Figure 4.** Diurnal universal time (UT) distribution of hourly number of DstMin in Kyoto Dst (blue) and USGS Dst (red) obtained separately for solar cycles 19–23.

be discussed in Section 4.2 using the other indices that use up to 15 stations and 4 satellites covering the Atlantic and Pacific.

To investigate further, the UT distribution of DstMin is considered separately for the five 11-year solar cycles (SCs) from 1958 to 2007. The distribution (Figure 4) shows clear quasi-semidiurnal variations in all SCs (19–23), though other periodic variations also seem to exist. To obtain the amplitudes (and phases) of the periodic variations, the data (Figure 4) are subjected to fast Fourier transform. Table 2 lists the amplitudes of the first four harmonics in the five SCs. The 12-hr component is stronger than other components in all SCs especially in the improved USGS Dst. In Kyoto Dst, the 8-hr component somehow becomes as strong as the 12-hr component in SC22 and slightly stronger in SC23. The phase is not listed in Table 2 for simplicity; it will be discussed in Section 4.2. The results (Figures 3 and 4 and Table 2) indicate that the quasi-diurnal variation could be reliable.

To check the effect of the hemispheric difference of the Dst stations, the UT distribution of DstMin is obtained separately for the four seasons which are considered to be 91 (and 92) days long centered at the equinoxes and solstices. The UT distribution in individual seasons (Figure 5) is similar to that obtained when all seasons are combined together indicating that the hemispheric difference of the Dst stations has only very little effect on the UT variation. The quasi-semidiurnal variation is clearer at equinoxes (Figures 5a and 5b) than in solstices. The minimum around 03–05 UT in June solstice (Figure 5c) and maximum around 06–08 UT in December solstice (Figure 5d) are not as pronounced as when all seasons are combined. Earlier, Mayaud (1978) also showed that the phase of the diurnal UT variation in Dst is independent of season.

**Table 2**
*Lists the Amplitudes of the First Four Harmonic Components of the Diurnal UT Distribution of DstMin in Kyoto Dst and USGS Dst in Five Solar Cycles (SC19–SC23)*

| Index | Harmonic components (hr) | SC19 | SC20 | SC21 | SC22 | SC23 |
|---|---|---|---|---|---|---|
| Kyoto | 24 | 2.91 | 2.43 | 1.69 | 3.35 | 2.54 |
| | 12 | 4.20 | 5.97 | 4.17 | 4.21 | 3.21 |
| | 8 | 2.51 | 1.95 | 0.33 | 4.21 | 4.02 |
| | 6 | 0.50 | 2.25 | 2.91 | 2.40 | 1.25 |
| USGS | 24 | 2.70 | 1.52 | 0.13 | 1.14 | 2.82 |
| | 12 | 4.06 | 3.71 | 4.05 | 4.13 | 2.82 |
| | 8 | 1.54 | 1.42 | 2.35 | 3.32 | 2.60 |
| | 6 | 1.25 | 1.58 | 1.50 | 0.58 | 0.50 |

The earlier study of the annual variation of the storms in the same two Dst indices showed a clear semiannual variation (Balan, Tulasiram, et al., 2017). The storms are now used to obtain their combined time-of-year/time-of-day plots simultaneously connecting both the diurnal UT and annual variations, which is found not exhibiting clear combined semiannual-semidiurnal patterns (not shown) due to insufficient number of storms. However, the number of stormy (Dst $\leq -50$ nT) hours (31,080 in Kyoto Dst and 18,177 in USGS Dst) are found to be sufficient. Figure 6 shows the annual and diurnal variations of these stormy hours

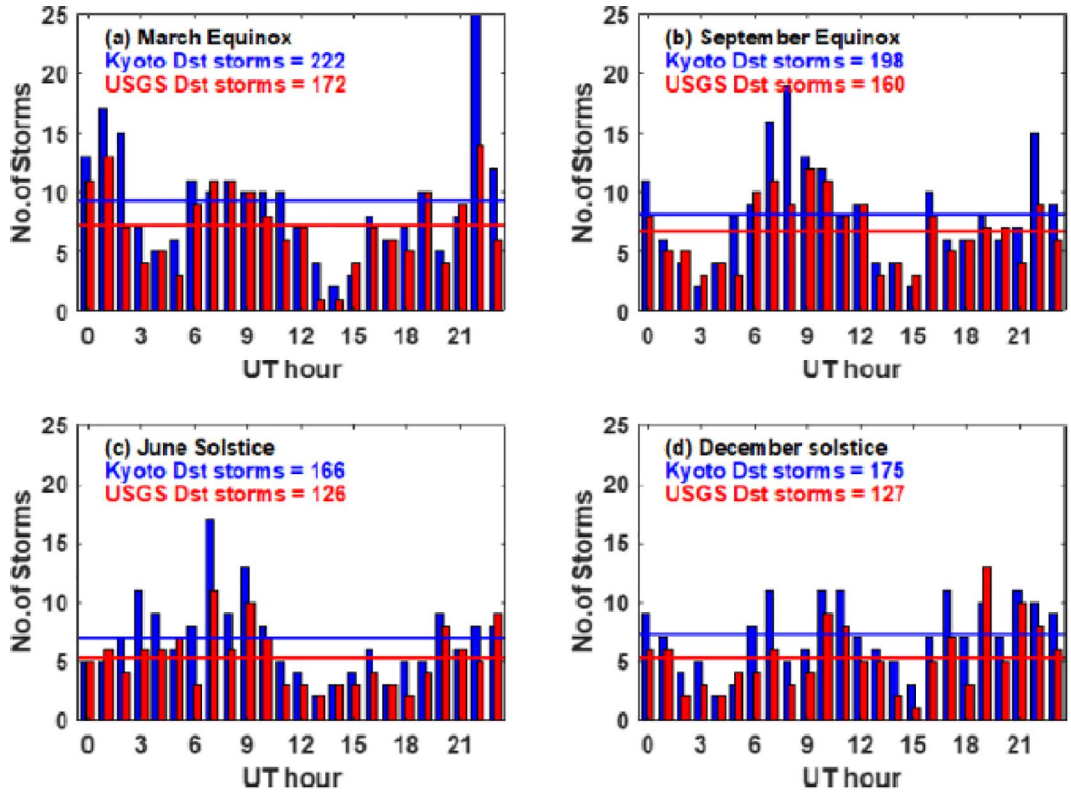


**Figure 5.** Diurnal universal time (UT) distribution of hourly number of DstMin in Kyoto Dst (blue) and USGS Dst (red) at March equinox (a), September equinox (b), June solstice (c), and December solstice (d).

by line curves and their combined time-of-year/time-of-day color plots for the two Dst indices. The combined plot exhibits clear maxima (and less clear minima) at the crossings of the expected seasons and UT hours. For example, maxima are seen in the 06–09 UT-April, 06–09 UT-October, 18–23 UT-April, and 18–23 UT-October bins.

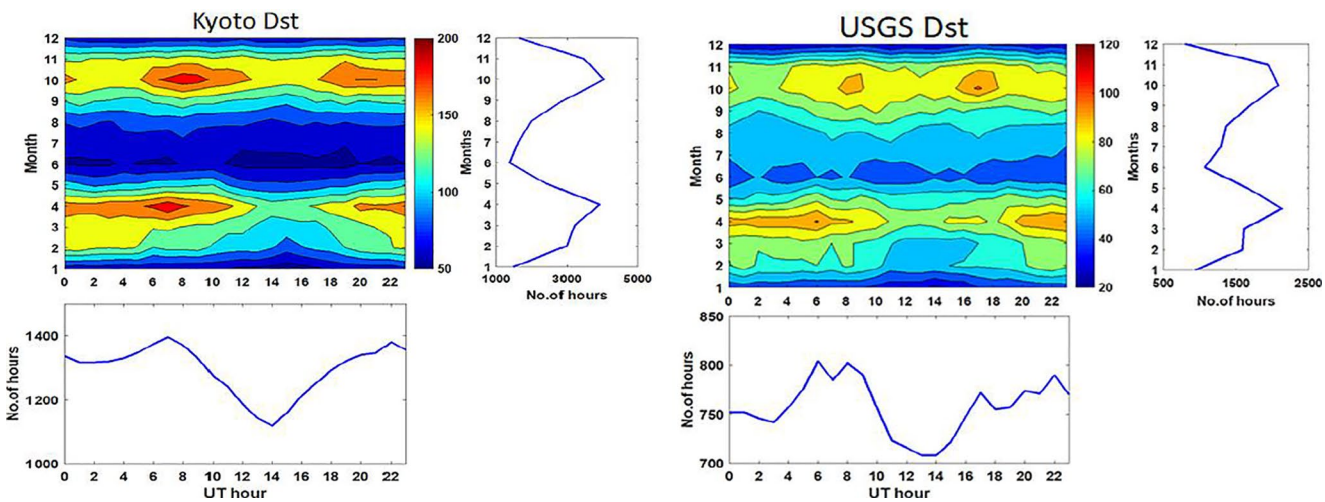


**Figure 6.** Monthly (vertical) and universal time (UT; horizontal) distributions of the number of stormy (Dst ≤ −50 nT) hours and their combined time-of-year/time-of-day plots in Kyoto Dst (left) and USGS Dst (right). The contours in the combined color plots (with no smoothing) and marginal distributions (line curves) are obtained directly from the data.

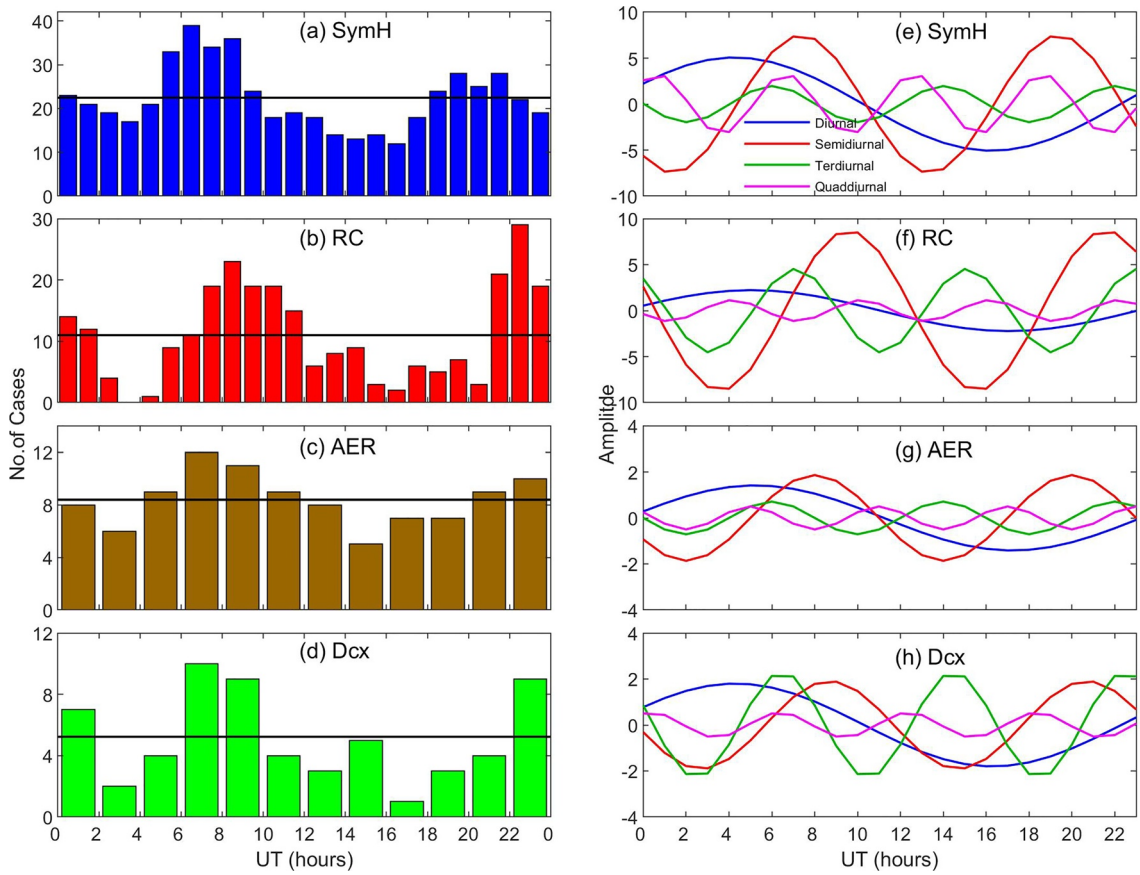


**Figure 7.** Diurnal universal time (UT) distribution of the storm intensity in SymH (a), ring current (RC) (b), Atmospheric and Environmental Research (AER) (c), and Dcx (d) indices; horizontal lines represent diurnal means. RHS panels (e), (f), (g), and (h) show the first four harmonic components in the respective indices.

### 4.2. Storm Statistics in Other Indices

Figure 7 shows the diurnal UT distribution of the storm intensity in the four indices with the right-hand panels displaying the first four harmonic components of the distributions in the left-hand panels. Hourly distribution is shown for the storms in 36 years in SymH index and 21 years in RC index; 2-hr distribution is used for the storms in 5 years in Dcx index and 7 years in AER index (Table 1). Irrespective of satellites or ground stations and their MLS, the quasi-semidiurnal variation is clear in the distribution of the storm intensity in all indices with maxima (around 06–08 UT and 21–23 UT) and minima (around 03–05 UT and 13–15 UT) occurring at around the same UT hours as the storm intensity distribution in Dst indices (Figure 3). The variation is clearer in the indices obtained using larger number of stations (SymH, RC, and Dcx). There is, however, slight difference in the exact UT hour for the occurrence of the maxima and minima in different indices. This may be due to the large differences in the number of storms in the indices and their time resolutions (1-min to 1-hr). As shown by the RHS panels (Figure 7), the 12-hr component is stronger than other components in all indices except in Dcx in which the 12-hr and 8-hr components have nearly equal amplitudes. Comparing the LHS and RHS blocks, it can also be seen that the phases of the peaks/dips of the 12-hr component correspond approximately to the maxima/minima in the distributions of the storm intensity in respective indices. The similar quasi-semidiurnal variations observed in all six indices therefore seem to indicate that the variation is real caused by some physical mechanisms, discussed in Section 5.

## 5. Discussion

A number of scientists studied the diurnal UT variation of low latitude geomagnetic storms using mainly Kyoto Dst (Ahn et al., 2002; Mayaud, 1978; Saroso et al., 1993; Siscoe & Crooker, 1996; Takalo et al., 1995). Recently, Yakovchouk et al. (2012) using the Dst storms in 1932–2009 reported that the UT hour of DstMin is determined mostly by the hour of maximum disturbance at ∼18 LT (local time) in one of the Dst stations. This seems to suggest that the reported quasi-semidiurnal variation (e.g., Ahn et al., 2002; Saroso et al., 1993) is apparent due to the uneven longitude and latitude distributions of the four Dst stations (e.g., Mayaud, 1978; Takalo & Mursula, 2001). The reported quasi-semidiurnal variation has also been interpreted (Saroso et al., 1993) in terms of the physical mechanisms such as equinoctial hypothesis (Bartels, 1932) and RM effect (Russell & McPherron, 1973). It has therefore become interesting to study the diurnal UT variation of the low latitude storms further for the conflicting real or apparent nature of the quasi-semidiurnal variation. We have undertaken such a study.

Unlike earlier studies, in this study, we have presented the diurnal UT variation using six low latitude indices. A computer program identified the storms by using four selection criteria that minimize nonstorm-like fluctuations. The UT variation is presented for the distribution of the storm intensity DstMin in the widely used Kyoto Dst (Sugiura, 1964; Sugiura & Kamei, 1991) and new and improved USGS Dst (Love & Gannon, 2009) in 50 years (1958–2007) together and separately for the four seasons and five 11-year solar cycles, both obtained using the data from four low latitude stations having MLS ∼120°. The other indices include SymH (Iyemori et al., 1992) in 36 years, RC (Finlay et al., 2012) in 20 years, Dcx (Karinen & Mursula, 2005) in 5 years and AER in 7 years. These indices use 12, 14, and 15 ground stations having MLS ∼70°, 110°, and 50° and four DMSP satellites, respectively.

The important results include (a) the diurnal UT distribution of the storm intensity in all six indices exhibits a striking quasi-semidiurnal type variation with maxima around 06–08 UT and 21–23 UT and minima around 03–05 UT and 13–15 UT (Figures 3–7). The variation present in all solar cycles (Figure 4) is clearer at equinoxes than in solstices (Figure 5). (b) The combined time-of-year/time-of-day plot of the stormy (Dst ≤ −50 nT) hours exhibits clear maxima at the crossings of the expected seasons and UT hours (Figure 6), though the same is not clear in the combined plot of the storms due to insufficient number of storms. These results imply that the quasi-semidiurnal variation of the low latitude storms is real caused by some physical mechanisms that become effective during storms.

### 5.1. Interpretation

As mentioned in Section 1, the equinoctial hypothesis (Bartels, 1932) and RM effect (Russell & McPherron, 1973) have been considered as potential mechanisms for the quasi-semidiurnal variation. Both the mechanisms are explained in terms of enhanced solar wind-magnetosphere coupling efficiency when the planet's dipole axis makes optimum angle with the streaming-in solar wind magnetic field (IMF) vector. The Earth's dipole axis makes a tilt of ∼11.1° with respect to its rotation axis which in turn is tilted by ∼23.5° with respect to solar ecliptic plane. Further, the geocentric solar ecliptic (GSE) plane is tilted by ∼7.25° with respect to geocentric solar equatorial (GSEQ) plane. As mentioned in Section 1, the equinoctial hypothesis is mainly based on the varying tilt angle $\mu$ between the Earth's dipole axis and GSE $Z$-axis in the $X$-$Z$ plane where $X$ points toward the center of the Sun from Earth (see Figure 3 in Lockwood, Owens, et al., 2020). On the other hand, the RM effect is based on the varying tilt angle $\theta$ of the dipole axis with respect to GSEQ $Z$-axis in the orthogonal plane to the Sun-Earth line. Both these angles ($\mu$ and $\theta$) vary with time-of-day (UT) and day-of-year. Figure 8 shows the time-of-year/time-of-day plots of $\mu$ and $\theta$ simultaneously combining their diurnal UT and annual variations. Such combined plots were presented and the mechanisms of the equinoctial hypothesis and RM effect were explained earlier (e.g., O'Brien & McPherron, 2002). Recently, Lockwood, McWilliams, et al. (2020) and Lockwood, Owens, et al. (2020) reported that RM mechanism is the central driver of geomagnetic storms. However, its effect on solar wind power input into the magnetosphere is small and there is a nonlinear amplification of the semiannual and UT variations in the geomagnetic response. This amplification is associated with solar wind dynamic pressure and its role in squeezing the near-Earth tail and so modulating the storage and release of the energy extracted from the solar wind.

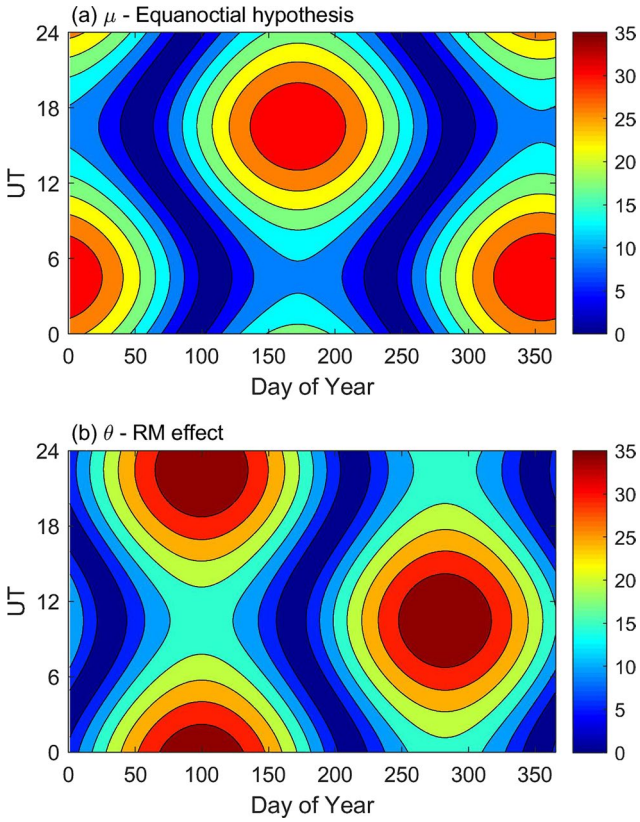


**Figure 8.** Combined time-of-year/time-of-day plots simultaneously connecting diurnal universal time (UT) and monthly variations of the dipole tilt angles $\mu$ involved in equinoctial hypothesis (a) and $\theta$ involved in Russell-McPherron (RM) effect (b).

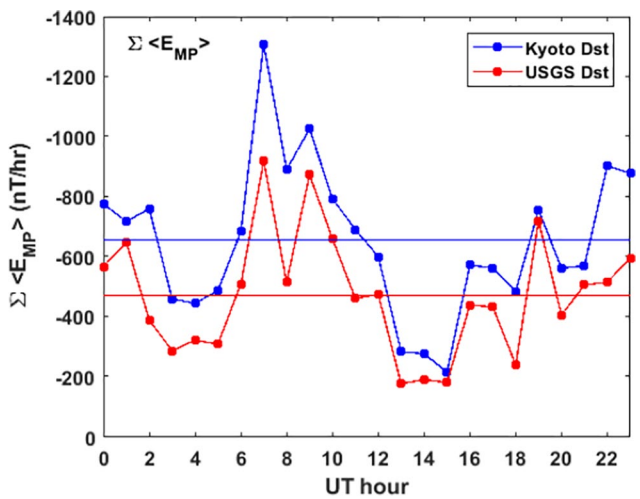


**Figure 9.** Diurnal universal time (UT) variation of mean energy input in the ring current during storm main phase (MP) computed using Kyoto Dst (blue) and USGS Dst (red) in 1958–2007.

Here, we try to interpret the observed UT variation in terms of its potential mechanisms. It was shown that the dayside magnetic reconnection maximizes at minimum values of $\mu$ (Borovsky et al., 2008; Cnossen et al., 2012; Siscoe & Crooker, 1996), and thereby controls the intensity and strength of geomagnetic storms. Russell et al. (2003) have shown that the neutral line ($X$-line) length, where the dayside reconnection occurs, extends to a larger longitudinal sector of ~170° when the angle $\mu$ is zero, and shrinks with the increase of $|\mu|$. On the other hand, the average Parker spiral of solar wind presents a significant antiparallel IMF component to the Earth's dipole field when the angle $\theta$ is nonzero. The angle $\theta$ maximizes during the equinoxes as can be seen from Figure 8b. During the spring equinox, the IMF toward the Sun ($B_{YGSEQ} < 0$) projects an antiparallel component onto the dipole axis, while the IMF away from the Sun ($B_{YGSEQ} > 0$) projects an antiparallel component on the dipole axis (Lockwood, Owens, et al., 2020; O'Brien & McPherron, 2002; Russell & McPherron, 1973). The IMF $B_{YGSEQ}$ component projects a larger antiparallel component on dipole axis for higher values of $\theta$ and causes enhanced dayside reconnection and transfer of solar wind energy into the magnetosphere. Frequent occurrence of the storms and larger storm intensity are therefore expected to be observed for absolute smaller values of $\mu$ and higher values of $\theta$ due to enhanced energy transfer from solar wind to the magnetosphere.

The rate of ring current development during MP, which is proportional to the rate of main energy input in the ring current (Burton et al., 1975), estimated from the Dst indices (Figure 9) exhibits a similar quasi-semidiurnal variation as the storm parameters, which further confirms the role of dipole tilt angle variation on the rate of reconnection and geomagnetic activity. Earlier, based on the UT variation of the energy input, Saroso et al. (1993) also suggested that the UT variation of Dst is not the effect of the index itself but the actual UT variation in the efficiency of solar wind-magnetosphere coupling.

Figure 10 shows the diurnal UT variations of the annual mean angles $\mu$ and $\theta$ superposed with the storm intensity distributions in Kyoto Dst and RC index during the common period 1997–2017. Both angles ($\mu$ and $\theta$) and storm intensity distributions show similar semidiurnal variations. The minima/maxima of the angle $\mu$ correspond approximately to the maxima/minima in the distributions (Figures 10a and 10c); and the minima/maxima of the angle $\theta$ correspond approximately to the minima/maxima in the distributions (Figures 10b and 10d). The magnitudes of the correlations of the intensity distributions with both angles $\mu$ and $\theta$ are high for both indices (~0.70 in RC and 0.62 in Kyoto Dst), indicating that the equinoctial hypothesis or RM effect or their combination could probably account for the quasi-semidiurnal variations of the storms. The small difference in the storm intensity distributions from the quasi-semidiurnal patterns observed in solstices (Figure 5) may be due to the tilt angles undergoing more of diurnal than semidiurnal variation in solstices. The quasi-semidiurnal variation of the storms observed in all indices and its association with the main energy input and possible mechanisms (equinoctial hypothesis and RM effect) indicate that the quasi-semidiurnal variation is real. This variation in the low latitude geomagnetic activity can be mainly ascribed to the variations of dipole tilt angles $\mu$ and $\theta$ and their role on the dayside reconnection rate.

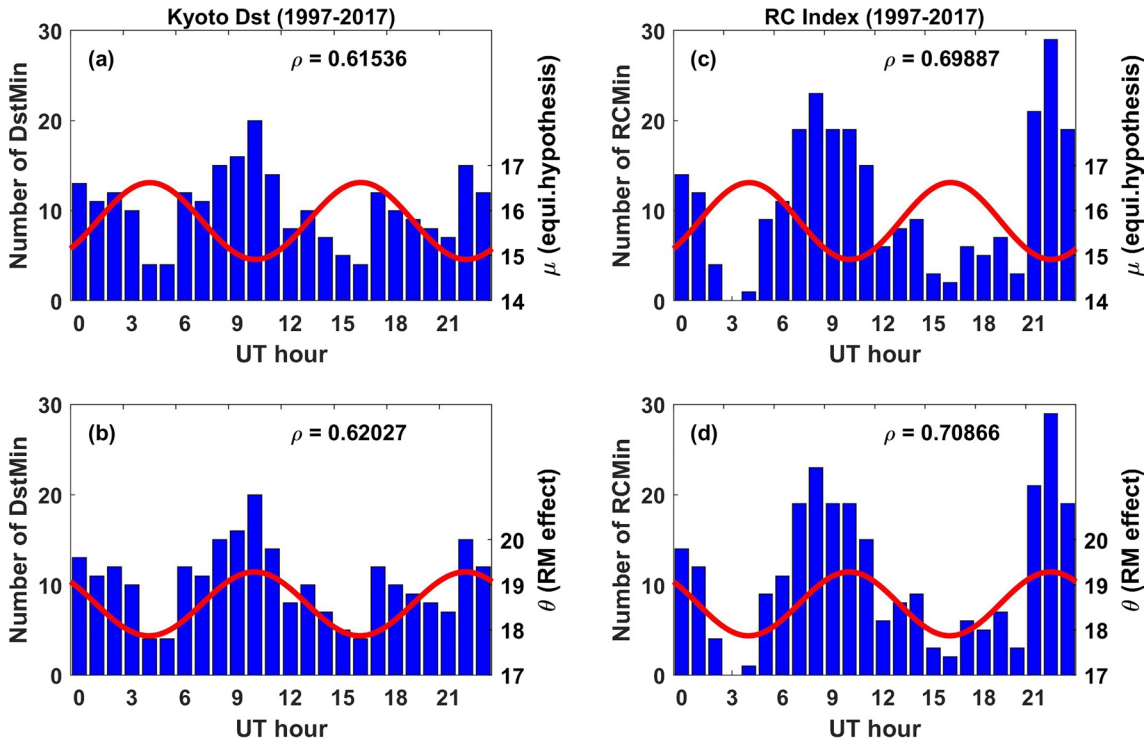


**Figure 10.** Universal time (UT) variations of yearly mean Earth's dipole tilt angles $\mu$ (a, b) and $\theta$ (c, d) superposed with that of the distribution of the storm intensity in Kyoto Dst (left) and ring current (RC) index (right).

The storm intensity (e.g., DstMin) is known to occur at the time when the ring current decay rate just takes over its growth-rate. The substorm current wedge and disruption of tail currents in the midnight sector during substorms could have a positive effect on the H-component, which gives a similar effect to the ring current decay (opposite effect to the ring current growth). However, this effect could statistically be almost equal in all longitudes. In other words, the statistically observed quasi-semidiurnal variation of the storm intensity could be caused by some physical mechanism such as equinoctial hypothesis or RM effect or their combination as discussed with Figure 10. Modeling studies are required to prove it, which is beyond the scope of the present study.

## 6. Summary

The diurnal UT variation of the geomagnetic storms observed in six available low latitude indices is presented. The indices include the Kyoto Dst, USGS Dst, RC, SymH, Dcx, and AER obtained from the H-component magnetic field measured at 4, 4, 14, 12, and 15 ground stations and four DMSP satellites, respectively, in 50, 50, 21, 36, 5, and 7 years. The ground stations used for deriving the indices have maximum longitude separations of ~120°, 120°, 110°, 70°, and 50°, respectively, and they are distributed with 3, 3, 11, 10 and 10 stations in the norther hemisphere and 1, 1, 3, 2, and 5 stations in the southern hemisphere.

A computer program using four selection criteria identified 761, 585, 258, 535, 61, and 97 storms (intensity $\leq -50$ nT) in the six indices, respectively, in 50, 50, 21, 36, 5, and 7 years. The UT variation of the important parameters such as the distribution of the storm intensity (DstMin) and values of main energy input in the ring current computed from Dst are presented for Kyoto Dst and USGS Dst. For other indices, the UT distribution of the storm intensity alone is shown.

The UT distribution of the storm intensity shows a striking quasi-semidiurnal type variation with maxima around 06–08 UT and 21–23 UT and minima around 03–05 UT and 13–15 UT in all indices, which is clearer in the indices using larger number of stations and at equinoxes. In the 50-year Kyoto Dst and USGS Dst data, the quasi-semidiurnal variation is observed in all five solar cycles and four seasons. Similar

variation is also observed in the UT variation of the main energy input in the ring current estimated from Dst. The quasi-semidiurnal variation associates well with the mechanisms of equinoctial hypothesis and Russell-McPherron effect. These observations indicate that the statistically observed quasi-semidiurnal variation of the low latitude geomagnetic storm intensity is real.

## Data Availability Statement

The authors thank the teams at Kyoto WDC and USGS for the Dst data available at http://wdc.kugi.kyoto-u.ac.jp/dstdir/ and geomag.usgs.gov/data, respectively. The authors also thank the teams of the SymH index available at http://wdc.kugi.kyoto-u.ac.jp/aeasy, RC index available at http://www.spacecenter.dk/files/magnetic-models/RC/, Dcx index available at http://dcx.oulu.fi/?link=queryProvisional, and AER index available at https://www.aer.com/science-research/space/space-weather/space-weather-index/. The derived parameters of the geomagnetic storms in Kyoto Dst (Table S1) and USGS Dst (Table S2) are available as Kyoto_Dst_Storms.txt and USGS_Dst_Storms.txt at https://zenodo.org/record/5568998.

**Acknowledgments**
This research has been supported by the National Natural Science Foundation of China (Grants 42120104003, 41874170, 41604139), the Foundation of China Research Institute of Radiowave Propagation (Grant A132101W02), and Chinese Meridian Project, and the foundation of National Key Laboratory of Electromagnetic Environment (Grants 6142403180103, 6142403180102). The authors would like to thank the two anonymous referees for their excellent reviews that have improved some parts of the paper.

## References

Ahn, B.-H., Moon, G.-H., Sun, W., Akasofu, S.-I., Chen, G. X., & Park, Y. D. (2002). Universal time variation of the Dst index and the relationship between the cumulative AL and Dst indices during geomagnetic storms. *Journal of Geophysical Research*, *107*(A11), 1409. https://doi.org/10.1029/2002JA009257

Akasofu, S.-I. (1981). The energy coupling between the solar wind and the magnetosphere. *Space Science Reviews*, *28*(121), 1981. https://doi.org/10.1007/bf00218810

Azpilicueta, F., & Brunini, C. (2012). A different interpretation of the annual and semiannual anomalies on the magnetic activity over the Earth. *Journal of Geophysical Research*, *117*, A08202. https://doi.org/10.1029/2012JA017893

Balan, N., Ebihara, Y., Skoug, R., Shiokawa, K., Batisa, I. S., TulasiRam, S., et al. (2017). A scheme for forecasting severe space weather. *Journal of Geophysical Research: Space Physics*, *122*, 2824–2835. https://doi.org/10.1002/2016JA023853

Balan, N., Skoug, R., Tulasi Ram, S., Rajesh, P. K., Shiokawa, K., Otsuka, Y., et al. (2014). CME front and severe space weather. *Journal of Geophysical Research: Space Physics*, *119*, 10041–10058. https://doi.org/10.1002/2014JA020151

Balan, N., Tulasiram, S., Kamide, Y., Batista, I. S., Souza, J. R., Shiokawa, K., et al. (2017). Automatic selection of Dst storms and their seasonal variations in two versions of Dst in 50 years. *Earth, Planets and Space*, *69*, 59. https://doi.org/10.1186/s40623-017-0642-2

Balan, N., Zhang, Q.-H., Shiokawa, K., Skoug, R., Xing, Z., Tulasi Ram, S. & Otsuka, Y. (2019). IpsDst of Dst storms applied to ionosphere-thermosphere storms and low latitude aurora. *Journal of Geophysical Research: Space Physics*, *124*, 9552–9565. https://doi.org/10.1029/2019JA027080

Balan, N., Zhang, Q.-H., Xing, Z.-Y., Skoug, R., Shiokawa, K., Lühr, H., et al. (2019). Capability of geomagnetic storm parameters to identify severe space weather. *The Astrophysical Journal*, *887*, 51. https://doi.org/10.3847/1538-4357/ab5113

Bartels, J. (1932). Terrestrial-magnetic activity and its relation to solar phenomena. *Terrestrial Magnetism and Atmospheric Electricity*, *37*(1), 1–52. https://doi.org/10.1029/TE037i001p00001

Borovsky, J. E., Hesse, M., Birn, J., & Kuzentsova, M. M. (2008). What determines the reconnection rate at the dayside magnetosphere? *Journal of Geophysical Research*, *113*, A07210. https://doi.org/10.1029/2007JA012645

Burton, R. K., McPherron, R. L., & Russell, C. T. (1975). An empirical relationship between interplanetary conditions and Dst. *Journal of Geophysical Research*, *80*(31), 4204–4214. https://doi.org/10.1029/JA080i031p04204

Cnossen, I., Wiltberger, M., & Ouellette, J. E. (2012). The effects of seasonal and diurnal variations in the Earth's magnetic dipole orientation on solar wind-magnetosphere-ionosphere coupling. *Journal of Geophysical Research*, *117*, A11211. https://doi.org/10.1029/2012JA017825

Cortie, A. L. (1912). Sunspots and terrestrial magnetic phenomena, 1898-1911: The cause of the annual variation in magnetic disturbances. *Monthly Notices of the Royal Astronomical Society*, *73*, 52–60. https://doi.org/10.1093/mnras/73.1.52

Daglis, I. A. (1997). The role of magnetosphere-ionosphere coupling in magnetic storm dynamics. In B. T. Tsurutani, W. D. Gonzalez, Y. Kamide, & J. K. Arballo (Eds.), *Magnetic storms. Geophysical Monograph Series* (Vol. 98, pp. 107–116). AGU. https://doi.org/10.1029/GM098p0107

Ebihara, Y., Fok, M.-C., Sazykin, S., Thomsen, M. F., Hairston, W. R., Evans, D. S., et al. (2005). Ring current and the magnetosphere-ionosphere coupling during the super storm of 20 November 2003. *Journal of Geophysical Research*, *110*, A09S22. https://doi.org/10.1029/2004JA010924

Ellis, W. (1899). On the relation between magnetic disturbance and the period of solar spot frequency. *Monthly Notices of the Royal Astronomical Society*, *60*, 142–157. https://doi.org/10.1093/mnras/60.2.142

Finlay, C. C., Jackson, A., Gillet, N., & Olsen, N. (2012). Core surface magnetic field evolution 2000–2010. *Geophysical Journal International*, *189*, 761–781. https://doi.org/10.1111/j.1365-246x.2012.05395.x

Gonzalez, W. D., Joselyn, J. A., Kamide, Y., Kroehl, H. W., Rostoker, G., Tsurutani, B. T., & Vasyliunas, V. M. (1994). What is a geomagnetic storm? *Journal of Geophysical Research*, *99*(A4), 5771–5792. https://doi.org/10.1029/93JA02867

Gopalswamy, N., Yashiro, S., Michalek, G., Xie, H., Lepping, R. P., & Howard, R. A. (2005). Solar source of the largest geomagnetic storm of cycle 23. *Geophysical Research Letters*, *32*, L12S09. https://doi.org/10.1029/2004GL021639

Iyemori, T. (1980). Time delay of the substorm onset from the IMF southward turning. *Journal of Geomagnetism and Geoelectricity*, *32*, 267–273. https://doi.org/10.5636/jgg.32.267

Iyemori, T., Araki, T., Kamei, T., & Takeda, M. (1992). *Midlatitude geomagnetic indices ASY and SYM (provisional No. 1 1989)*. Kyoto University.

Karinen, A., & Mursula, K. (2005). A new reconstruction of the Dst index for 1932–2002. *Annales Geophysicae*, *23*, 475–485. https://doi.org/10.5194/angeo-23-475-2005

Katus, R. M., & Liemohn, M. W. (2013). Similarities and differences in low-to middle-latitude geomagnetic indices. *Journal of Geophysical Research: Space Physics*, *118*, 5149–5156. https://doi.org/10.1002/jgra.50501

Liemohn, M. W., Kozyra, J. U., Thomsen, M. F., Roeder, J. L., Lu, G., Borovsky, J. E., & Cayton, T. E. (2001). Dominant role of the asymmetric ring current in producing the storm time Dst*. *Journal of Geophysical Research*, *106*(10), 883. https://doi.org/10.1029/2000JA000326

Lockwood, M., McWilliams, K. A., Owens, M. J., Barnard, L. A., Watt, C. E., Scott, C. J., et al. (2020). Semi-annual, annual and universal time variations in the magnetosphere and in geomagnetic activity: 2. Response to solar wind power input and relationships with solar wind dynamic pressure and magnetospheric flux transport. *Journal of Space Weather and Space Climate*, *10*, 30. https://doi.org/10.1051/swsc/2020033

Lockwood, M., Owens, M. J., Barnard, L. A., Haines, C., Scott, C. J., McWilliams, K. A., & Coxon, J. C. (2020). Semi-annual, annual and universal time variations in the magnetosphere and in geomagnetic activity: 1. Geomagnetic data. *Journal of Space Weather and Space Climate*, *10*, 23. https://doi.org/10.1051/swsc/2020023

Love, J. J., & Gannon, J. L. (2009). Revised Dst and the epicycles of magnetic disturbance: 1958–2007. *Annales Geophysicae*, *28*(8), 3101–3131. https://doi.org/10.5194/angeo-27-3101-2009

Lühr, H., Xiong, C., Olsen, N., & Le, G. (2017). Near-Earth magnetic field effects of large-scale magnetospheric currents. *Space Science Reviews*, *206*(1–4), 521–545. https://doi.org/10.1007/s11214-016-0267-y

Lyatsky, W., Newell, P. T., & Hamza, A. (2001). Solar illumination as cause of the equinoctial preference for geomagnetic activity. *Geophysical Research Letters*, *28*(12), 2353–2356. https://doi.org/10.1029/2000GL012803

Mayaud, P. N. (1978). The annual and daily variations of the Dst index. *Geophysical Journal International*, *55*, 193–201. https://doi.org/10.1111/j.1365-246x.1978.tb04757.x

Newell, P. T., Meng, C.-I., Sotireli, T., & Liou, K. (2001). Polar Ultraviolet Imager observations of global aurora power as a function of polar cap size and magnetotail stretching. *Journal of Geophysical Research*, *106*(A4), 5895–5905. https://doi.org/10.1029/2000JA003034

O'Brien, T. P., & McPherron, R. L. (2000). An empirical phase space analysis of ring current dynamics: Solar wind control of injection and decay. *Journal of Geophysical Research*, *105*(A4), 7707–7719. https://doi.org/10.1029/1998JA000437

O'Brien, T. P., & McPherron, R. L. (2002). Seasonal and diurnal variation of Dst dynamics. *Journal of Geophysical Research*, *107*(A11), 1341. https://doi.org/10.1029/2002JA009435

Olsen, N., Sabaka, T. J., & Lowes, F. (2005). New parameterization of external and induced fields in geomagnetic field modeling, and a candidate model for IGRF 2005. *Earth, Planets and Space*, *57*, 1141–1149. https://doi.org/10.1186/BF03351897

Richardson, I. G., Cliver, E. W., & Cane, H. V. (2001). Sources of geomagnetic storms for solar minimum and maximum conditions during 1972–2000. *Geophysical Research Letters*, *28*(13), 2569–2572. https://doi.org/10.1029/2001GL013052

Rostoker, G., Samson, J. C., Creutzberg, F., Hughes, T. J., McDiarmid, D. R., McNamara, A. G., et al. (1995). CANOPUS: A ground based instrument array for remote sensing the high latitude ionosphere during the ISTP/GGS program. *Space Science Reviews*, *46*, 743–760. https://doi.org/10.1007/BF00751349

Russell, C. T., & Mcpherron, R. L. (1973). Semiannual variation of geomagnetic activity. *Journal of Geophysical Research*, *78*(1), 92–108. https://doi.org/10.1029/JA078i001p00092

Russell, C. T., Wang, Y. L., & Raeder, J. (2003). Possible dipole tilt dependence of dayside magnetopause reconnection. *Geophysical Research Letters*, *30*(18), 1937. https://doi.org/10.1029/2003GL017725

Sabine, E. (1856). On the periodical laws discoverable in the mean effects of the large geomagnetic disturbances. *Philosophical Transactions of the Royal Society, London*, *146*, 357.

Saroso, S., Iyemori, T., & Sugiura, M. (1993). Universal time variations in the ap and Dst indices and their possible cause. *Journal of Geomagnetism and Geoelectricity*, *45*, 563–572. https://doi.org/10.5636/jgg.45.563

Siscoe, G., & Crooker, N. (1996). Diurnal oscillation of Dst: A manifestation of the Russell-McPherron effect. *Journal of Geophysical Research*, *101*(A11), 24985–24989. https://doi.org/10.1029/96JA01875

Sugiura, M. (1964). Hourly values of equatorial Dst for the IGY. *Annals of the International Geophysical Year*, *35*, 9–45.

Sugiura, M., & Kamei, T. (1991). Equatorial Dst index 1957–1986. In A. Berthelier, & M. Menvielle (Eds.), *IAGA Bullet, 40*. International Service of Geomagnetic Indices.

Svalgaard, L. (1977). Geomagnetic activity: Dependence on solar wind parameters. In J. B. Zirker (Ed.), *Coronal holes and high speed wind streams* (pp. 371–441). Colorado Association of University Press.

Svalgaard, L. (2011). Geomagnetic semiannual variation is not overestimated and is not an artifact of systematic solar hemispheric asymmetry. *Geophysical Research Letters*, *38*, L16107. https://doi.org/10.1029/2011GL048616

Takalo, J., Lohikoski, R., & Timonen, J. (1995). Structure function as a tool in AE and Dst time series analysis. *Geophysical Research Letters*, *22*(5), 635–638. https://doi.org/10.1029/95GL00053

Takalo, J., & Mursula, K. (2001). A model for the diurnal universal time variation of the Dst index. *Journal of Geophysical Research*, *106*(A6), 10905–10914. https://doi.org/10.1029/2000JA000231

Tulasi Ram, S., Liu, C. H., & Su, S.-Y. (2010). Periodic solar wind forcing due to recurrent coronal holes during 1996–2009 and its impact on Earth's geomagnetic and ionospheric properties during the extreme solar minimum. *Journal of Geophysical Research*, *115*, A12340. https://doi.org/10.1029/2010JA015800

Vijaya Lekshmi, D., Balan, N., Tulasi Ram, S., & Liu, J. Y. (2011). Statistics of geomagnetic storms, and ionospheric storms at low and mid latitudes in two solar cycles. *Journal of Geophysical Research*, *116*, A11328. https://doi.org/10.1029/2011JA017042

Yakovchouk, O. S., Mursula, K., Holappa, L., Veselovsky, I. S., & Karinen, A. (2012). Average properties of geomagnetic storms in 1932–2009. *Journal of Geophysical Research*, *117*, A03201. https://doi.org/10.1029/2011JA017093

Zhang, J., Richardson, I. G., Webb, D. F., Gopalswamy, N., Huttunen, E., Kasper, J. C., et al. (2007). Solar and interplanetary sources of major geomagnetic storms (Dst < −100 nT) during 1996–2005. *Journal of Geophysical Research*, *112*, A10102. https://doi.org/10.1029/2007JA012321

Zhao, H., & Zong, Q.-G. (2012). Seasonal and diurnal variation of geomagnetic activity: Russel-McPherron effect during different IMF polarity and/or extreme solar wind condition. *Journal of Geophysical Research*, *117*, A11222. https://doi.org/10.1029/2012JA017845